J Bioenerg Biomembr (2009) 41:369–377
DOI 10.1007/s10863-009-9236-4

Mitochondrial damage as death inducer in heart-derived H9c2 cells: more than one way for an early demise

Antonio Lax · Fernando Soler · Francisco Fernández-Belda

Received: 14 July 2009 / Accepted: 28 July 2009 / Published online: 24 September 2009

Abstract The release of cytochrome c from mitochondria induced by 10 μM thapsigargin was linked to rapid loss of the mitochondrial membrane potential whereas that induced by 50 nM staurosporine was mediated by Bax activation and occurred in polarized mitochondria. Similar levels of cytochrome c were observed when induced by either thapsigargin or staurosporine indicating that the release magnitude was independent of the mechanism involved in membrane permeabilization. In any case caspase 3 activation was subsequent to cytochrome c release. Mitochondrial dysfunction and release of cytochrome c occurred earlier when induced by thapsigargin even though morphological alteration of the cell and chromatin condensation were developed earlier in the presence of staurosporine. In addition, a general and irreversible caspase inhibitor did not protect against chromatin condensation induced by staurosporine. It is also shown that earlier mitochondrial damage does not always correlate with earlier cell demise. This can be attributed to the existence of alternative caspase-independent cell death programmes.

Keywords Staurosporine · Thapsigargin · Mitochondria · Cell death · Cardiomyocyte

Abbreviations

OMM	outer mitochondrial membrane
$\Delta\Psi_m$	mitochondrial membrane potential
PTP	permeability transition pore
cyt c	cytochrome c
ST	staurosporine
TG	thapsigargin
MTT	3-(4,5-dimethylthiazol-2-yl)-2,5-diphenyltetrazolium bromide
AO	acridine orange
CsA	cyclosporin A
DMEM	Dulbecco's modified Eagle's medium
JC-1	5,5′,6,6′,-tetrachloro-1,1′,3,3′-tetraethylbenzimidazolylcarbocyanine iodide
z-VAD-fmk	N-benzyloxycarbonyl-valinyl-alanilyl-aspartyl (O-methyl ester)-fluoromethylketone
PBS	phosphate-buffered saline
Hepes	4-(2-hydroxyethyl)piperazine-1-ethanesulfonic acid
PBST	phosphate-buffered saline supplemented with Tween-20
EGTA	ethylene glycol-bis(β-aminoethyl ether)-N,N,N',N'-tetraacetic acid
COX IV	cytochrome oxidase, complex IV
casp	caspase
Bax	Bcl-2-associated X protein

A. Lax · F. Soler · F. Fernández-Belda (✉)
Departamento de Bioquímica y Biología Molecular A,
Universidad de Murcia,
Campus de Espinardo,
30071 Murcia, Spain
e-mail: fbelda@um.es

Introduction

The mitochondrion is not only the power plant of the cell but also the site for other reactions of the intermediary metabolism and certain processes such as xenobiotics modification and Ca^{2+} regulation. This organelle is also the target of multiple pro-apoptotic signals and contains a number of effector proteins that can promote cell death (Kroemer and Reed 2000; Ferri and Kroemer 2003).

It has been suggested that the integrity of mitochondrial membranes is essential for cell life and permeabilization of

the OMM is regarded as a 'point of no return' in apoptotic cell death (Kroemer and Reed 2000). Numerous physiological and pathological agents can induce the process although the mechanism involved in the permeabilization is controversial (Green and Kroemer 2004). Current knowledge indicates that the OMM can be selectively permeabilized without alteration of $\Delta\Psi_m$ by the intervention of pro-apoptotic proteins of the Bcl-2 family. Alternatively, PTP opening can lead to $\Delta\Psi_m$ loss and matrix swelling that eventually causes rupture of the OMM. These two major mechanisms seem to be operative depending on cell model and apoptotic inducer.

In any case permeabilization of the OMM is ensued by translocation of apoptotic proteins including cyt c from the mitochondrial intermembrane space to the cytosol. The accumulation of cyt c in the cytosol varies from minutes to hours when measured in a cell population since the onset of release in each individual cell is a stochastic process. However, studies on the kinetics of cyt c release in single cells have revealed that the process is rapid and occurs in virtually all of the mitochondria (Goldstein et al. 2000; Goldstein et al. 2005) although this is at odds with keeping $\Delta\Psi_m$ and energy production. The presence of cyt c in the mitochondria of a subset of cells or re-entry into the intermembrane space has been suggested to explain experimental findings (Goldstein et al. 2000). Other studies have indicated that cyt c resides in two functionally distinct pools, a small fraction that is freely available and a large fraction that is sequestered in the intercristae compartments (Bernardi et al. 1999; Scorrano et al. 2002). Consequently, selective permeabilization of the OMM can only account for ~10–15 % of the total cyt c content with minimal impact on $\Delta\Psi_m$ and energy production. Swelling of the mitochondrial matrix and decrease of $\Delta\Psi_m$ (Bernardi et al. 1999) or transient PTP opening without $\Delta\Psi_m$ collapse and cristae remodeling (Scorrano et al. 2002) would be required for a larger release of cyt c. Different amplification loops have been proposed to explain the biphasic release of cyt c (Garrido et al. 2006). At this point it is unclear whether the amount of cyt c release is dependent on the OMM permeabilization mechanism and the real contribution of cyt c release and other molecular components to set in motion the apoptotic machinery. It is conceivable that the study of the overall kinetics and extent of cyt c release under different experimental settings would provide useful information to evaluate the impact of mitochondrial damage on the apoptotic process.

Myocardiac cells are endowed with a high content of mitochondria, equivalent to ~30% of the cellular volume, and maintain an elevated rate of ATP synthesis to satisfy the energy demand of the heart. This makes myocardiac cells highly vulnerable to mitochondrial damage (Regula et al. 2003). In fact, mitochondrial damage and the subsequent apoptotic process in cardiomyocytes have been consistently associated with several pathological conditions, including oxidative stress, hypoxia, ischemia-reperfusion and infarction (Regula et al. 2003).

The experimental mitochondrial damage has been induced by exposure of our cell model to ST, a broad-spectrum inhibitor of protein kinase that can elicit mitochondrion dependent apoptosis (Bossy-Wetzel et al. 1998; Heiskanen et al. 1999) or to TG, a high affinity inhibitor of Ca^{2+}–ATPase from sarcoplasmic reticulum (Sagara and Inesi 1991) with a fast and direct effect on the mitochondrion when used at a relatively high concentration (Vercesi et al. 1993; Korge and Weiss 1999; Lax et al. 2006). Biochemical and structural parameters related with apoptosis have been analyzed to gain new insights into the mitochondrion-mediated death of cardiomyocytes.

Materials and methods

Reagents TG, ST from *Streptomyces sp*., MTT, AO, CsA and the protease inhibitor cocktail were obtained from Sigma. Culture reagents including DMEM with low glucose and L-glutamine, fetal bovine serum, penicillin-streptomycin-L-glutamine mixture and the cell dissociation solution containing 0.25% trypsin were Gibco® brand products from Invitrogen. JC-1 was a Molecular Probes™ reagent from Invitrogen and the general caspase inhibitor z-VAD-fmk was from Bachem. Reagents for the protein assay were obtained from Pierce. All other chemicals were of analytical grade and provided by Sigma.

Experimental media The complete culture medium was DMEM supplemented with 10% heat-inactivated fetal bovine serum, 2 mM L-glutamine, 100 units/ml penicillin and 100 μg/ml streptomycin. PBS was 137 mM NaCl, 2.7 mM KCl, 10.14 mM Na_2HPO_4 and 1.76 mM KH_2PO_4 adjusted to pH 7.4 with HCl. The modified Tyrode's solution was 10 mM Hepes, 121 mM NaCl, 4.7 mM KCl, 1 mM $CaCl_2$, 1.2 mM $MgSO_4$, 5 mM $NaHCO_3$, 1.2 mM KH_2PO_4, 10 mM glucose and 0.25% bovine serum albumin adjusted at pH 7.4 with NaOH. The permeabilization medium for digitonin treatment was 250 mM sacarose, 75 mM KCl, 1 mM NaH_2PO_4 and 8 mM Na_2HPO_4. The solubilization medium after the digitonin treatment was 150 mM Tris, 1 mM EGTA, 1% Triton X-100, 1% sodium deoxycholate and 0.1% SDS adjusted at pH 8.0 with HCl. The sample buffer for electrophoresis was 78 mM Tris, 3% SDS, 5% β-mercaptoethanol, 10% glycerol and 0.015% bromophenol blue adjusted at pH 6.8 with HCl. PBST was PBS containing 0.05% Tween-20. The blocking solution for blotted proteins was PBST supplemented with 5% skim dried milk. The stripping buffer for antibody reprobing was

62.5 mM Tris, 100 mM β-mercaptoethanol and 2% SDS adjusted at pH 6.8 with HCl.

Materials H9c2 cells derived from embryonic rat heart (Kimes and Brandt 1976) were obtained from the European Collection of Cell Cultures (Salisbury, UK). Culture plates and coverslips were supplied by Sarstedt. The nitrocellulose transfer membrane Protran® BA 83 was a Schleicher & Schuell product from Whatman. Chemichrome Western Control and the Peroxidase Chemiluminescent kit (CPS-1) were obtained from Sigma. Qentix™ Western Blot Signal Enhancer was from Pierce and Curix RP2 plus film was a product of Agfa.

Cell culture H9c2 cells at low passage were cultured at 37°C in a water-saturated atmosphere containing 5% CO_2 and 95% air (Lax et al. 2005). The monolayer culture was resuspended and plated at a lower density (1:6) or harvested to carry out experiments when 70–80% confluence was reached. Myoblats were made quiescent before any treatment by changing the complete culture medium by DMEM. The mitochondrial damage was induced by the presence of 10 μM TG or 50 nM ST.

Mitochondrial reductase activity Cells were seeded in quadruplicate at ~15×10^3 cells/well in 24-well plates. Subconfluent cultures were washed twice with PBS at 37°C and then exposed in DMEM at 37°C for different time intervals to mitochondrial damage. The incubation medium from treated and non-treated cells was aspirated and cells were washed with PBS pre-warmed at 37°C. Cells in each well were incubated for 30 min with 300 μl of 1 mg/ml MTT in the CO_2 incubator. The colorimetric assay for evaluating MTT reduction was carried out as previously described (Soler et al. 2007). The index of cell survival at each time interval in the absence or presence of treatment corresponds to a percentage with respect to a control at zero time.

Morphological appearance Subconfluent cultures in 100-mm plates were washed twice with PBS at 37°C. Adherent cells in DMEM were exposed to treatment as described above. Cultures were washed twice with PBS at 37°C and then observed by phase contrast with a Leica DM IL inverted microscope. Images were collected with a Leica DC300 F digital camera using the software IM50 1.2 from Leica.

Chromatin detection Cells grown on 13-mm round plastic coverslips placed in 24-well plates were washed twice with PBS at 37°C. Exposure to the corresponding treatment was maintained for 1 or 2 h in the CO_2 incubator. Pretreatment for 1 h with 20 μM z-VAD-fmk was carried out when indicated. Adherent cells were fixed and stained with AO as previously described (Lax et al. 2006). Each coverslip was washed three times with pre-warmed PBS and inverted onto a glass slide containing Sigma mounting medium. Images were taken with a Leica DMRB epifluorescence microscope equipped with the I3 filters block. The digital camera was Leica DC500 and the software was IM50 (version 1.2).

$\Delta\Psi_m$ measurement Cells in one 150-mm plate at 70–80% confluence were washed twice with PBS pre-warmed at 37°C and then exposed for different time intervals to mitochondrial damage in DMEM at 37°C. When indicated, the 10 μM TG addition was preceded by 10 min preincubation with 5 μM CsA. Treated and untreated cells were loaded at 37°C for 10 min with 5 μg/ml JC-1. Then, cells were washed twice with PBS pre-warmed at 37°C and detached by trypsinization. Cells were resuspended (~3×10^5 cells/ml) in modified Tyrode's solution at 25°C and measurements were performed immediately. Samples were excited with a laser source tuned at 488 nm in a FACSort™ flow cytometer from Becton Dickinson. The green fluorescence of JC-1 was detected through the FL-1 channel and the red fluorescence through the FL-2 channel (Soler et al. 2007). Fluorescence spillover in the channels was corrected as previously described (Cossarizza et al. 1993). Measurements of forward *vs.* side light scatter were used to select the cell population under study. For the analysis of each sample, a total of 20,000 events at a rate of ~200 cells/s were collected. CellQuest™ software from Becton Dickinson was used for data acquisition and analysis.

Cellular extracts Subconfluent cultures in 4 × 150-mm plates (~$1.5–2\times10^6$ cells/plate) were washed twice with PBS pre-warmed at 37°C and then exposed to mitochondrial damage in DMEM at 37°C. Treated and untreated cells were maintained in the CO_2 incubator for different time intervals. In some experiments, cells were preincubated for 10 min with 5 μM CsA or 1 h with 20 μM z-VAD-fmk before exposure to mitochondrial damage. At the end of each incubation time, cells were trypsinized and sedimented by centrifugation at 480 ×g for 10 min and 4°C. Afterwards, cells were washed twice with ice-cold PBS, resuspended at ~ 4×10^4 cells/μl in ice-cold medium for permeabilization and supplemented with protease inhibitor cocktail at a proportion of 4 μl/1×10^6 cells. Selective permeabilization of the plasma membrane (Gottlieb and Granville 2002) was achieved by 5 min incubation on ice bath with 600 μg/ml digitonin. The digitonin concentration was previously adjusted to get Trypan blue staining in more than 95% of the cells. Then, cells were centrifuged at 10,000 ×g for 10 min and 4°C and the supernatant was aliquoted, labeled as "S-10 fraction" and stored at −80°C for further analysis. The resulting pellet was resuspended in

a volume of solubilization medium equal to the volume of medium for permeabilization used in the precedent step and supplemented with protease inhibitor cocktail at 4 μl/1×10^6 cells. The lysate was cleared by brief sonication, i.e., 4×5 s at 30 s intervals, followed by centrifugation at 10,000 ×g for 10 min and 4°C. The supernatant was aliquoted, labeled as "P-10 fraction" and stored at −80°C for further study. Cyt c was studied in the S-10 and P-10 fractions, Bax in the P-10 fraction and the S-10 fraction was used for caspase detection.

Protein determination Aliquots of whole cell lysate or cellular extracts were subjected to evaluation of protein content. The bicinchoninic acid method and bovine serum albumin as the standard protein were used (Smith et al. 1985).

Separation and detection of proteins Cellular extracts were loaded onto SDS-polyacrylamide minigels. Electrophoresis and Western blot analysis were performed as previously described (Soler et al. 2007), using mouse anti-cyt c monoclonal antibody (clone 7H8.2C12) from BD PharMingen™, mouse monoclonal antibody against COX IV from Molecular Probes™ (Invitrogen) and rabbit anti-casp 3 polyclonal antibody (H-277) from Santa Cruz Biotechnology. Mouse anti-Bax monoclonal antibody (clone 6A7), mouse monoclonal anti-γ-tubulin (clone GTU-88) and the peroxidase-conjugated secondary antibodies rabbit anti-mouse IgG and goat anti-rabbit IgG were from Sigma. Immunoreactive bands were detected by the peroxidase activity using Sigma chemiluminescence reaction and protocol. Blots related with casp 3 activation contain unspecific bands that are related with overexposure to detect proteolytic cleavage. Equal loading in the lanes was checked with the anti-γ-tubulin antibody.

Data presentation Experimental data in the histograms correspond to mean values of at least five independent assays and standard deviations are indicated by error bars. The significance of observed differences was analyzed by the Student's t-test using the SigmaPlot 8.0 software from Jandel Corporation. A value of $p<0.05$ was considered to be statistically significant. Cell images and protein blots are representative of repeated experiments and were reproduced using Adobe Photoshop 4.0. None or minimal image treatment according to accepted guidelines was applied (Rossner and Yamada 2004). Blots were quantified by laser scanning densitometry when indicated. Flow-cytometry data presented as dots plot correspond to representative experiments performed at selected assay conditions. Time-dependent plots contain mean values from at least three experiments and the results are expressed as percentage of the cell population under study.

Results

The incubation of plated cells in DMEM at 37°C with either 10 μM TG or 50 nM ST was accompanied by a time-dependent decrease in viability of the cell population as detected by measurements of MTT reduction. Thus, TG decreased 55% the reductase activity of mitochondria after 2 h of treatment and the functional damage approached to 100 % in ~6 h (Fig. 1a). Nevertheless, the mitochondrial function only decreased 30% after 2 h of ST treatment and the complete effect was developed when the treatment was prolonged for at least 8 h (Fig. 1b). The harmful effect

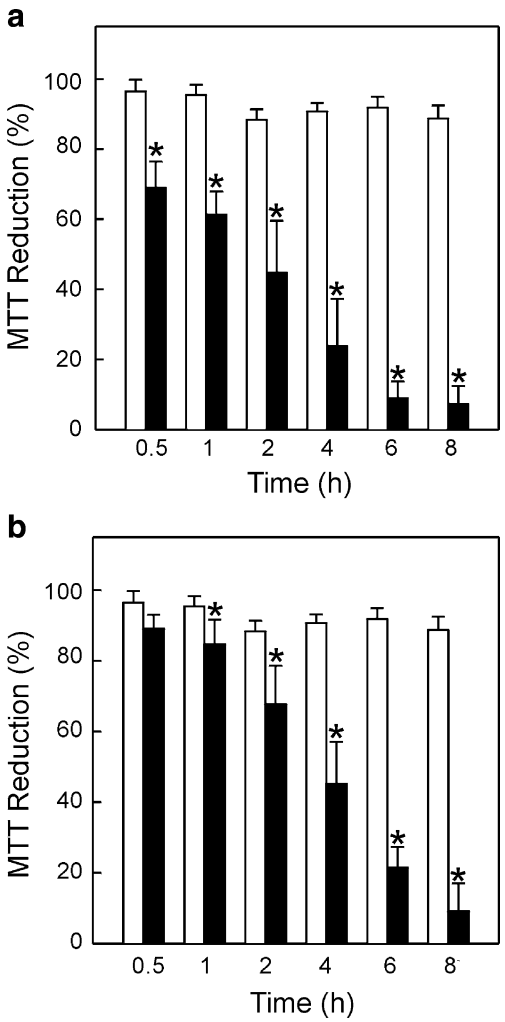

Fig. 1 Effect of mitochondrial damage inducers on mitochondrial function of H9c2 cells. Plated cells in DMEM at 37°C were exposed to 10 μM TG (**a**) or 50 nM ST (**b**) for different time periods (closed bars). Control experiments were performed by maintaining cells in DMEM at 37°C for the same time intervals but in the absence of treatment (open bars). Cell damage was evaluated with the MTT assay. Data are expressed as a percentage with respect to a time zero control. Asterisk indicates statistically significant difference between treated and untreated cells at the same incubation time

associated to serum removal was negligible due to the relatively short time scale of the experiments (Fig. 1).

The effect of TG or ST on the cell culture was then analyzed by measuring relevant parameters related with the apoptotic process. This was proved by Western blotting once digitonin was added to the cells and a differential centrifugation was performed to isolate cellular fractions. Cyt c was present in the P-10 fraction of typical control cultures but was absent in S-10, however 10 μM TG induced the time-dependent appearance of cyt c in S-10 (Fig. 2). The presence of cyt c in S-10 was first noticed at 30 min and tended to increase as a function of time. Blot reprobing with a specific antibody against COX IV indicated that mitochondria were present in the P-10 fraction but not in S-10. Furthermore, detection of γ-tubulin confirmed that samples in the same set of experiments had a similar protein content. Redistribution of cyt c from mitochondria to cytosol was also observed when 50 nM ST was added to the cells. In this case, the presence of cyt c in the S-10 fraction was observed after 1 h. Here again, the time-dependent appearance of cyt c in the S-10 fraction occurred when the γ-tubulin content revealed similar protein loading of the lanes.

JC-1 is a cationic probe that can be used to detect alterations in $\Delta\Psi_m$ (Cossarizza et al. 1993; Soler et al. 2007). The accumulation of JC-1 in the mitochondria of live cells leads to an increase in red fluorescence due to the formation of J-aggregates whereas a $\Delta\Psi_m$ fall is accompanied by a decrease in the red to green fluorescence ratio of the probe. Representative experiments indicated that the vast majority of untreated cells loaded with JC-1 displayed intense red fluorescence and a lower green fluorescence due to the presence of polarized mitochondria (Fig. 3a). Cells in region R1 were 87.4% *vs.* 12.6% in region R2. However, when cells were exposed to 10 μM TG for 2 h, there was a clear decrease in red fluorescence that was accompanied by an increase in green fluorescence (Fig. 3b). After the TG treatment, cells in regions R1 and R2 were 0.7% and 99.3%, respectively. Notably, a large proportion of the cells maintained high red fluorescence when preincubated for 10 min with 5 μM CsA before the 10 μM TG treatment (Fig. 3c). Cells in region R1 were now 84.1% and cells in R2 were 15.9%. The effect of ST on $\Delta\Psi_m$ was also evaluated by the same procedure. Our data indicated that the bivariate plot of the JC-1 fluorescence was very similar to that of untreated cells (Fig. 3a) when cells were exposed to 50 nM ST for 2 h (Fig. 3d). A more complete picture emerged by studying the time course of the JC-1 fluorescence response.

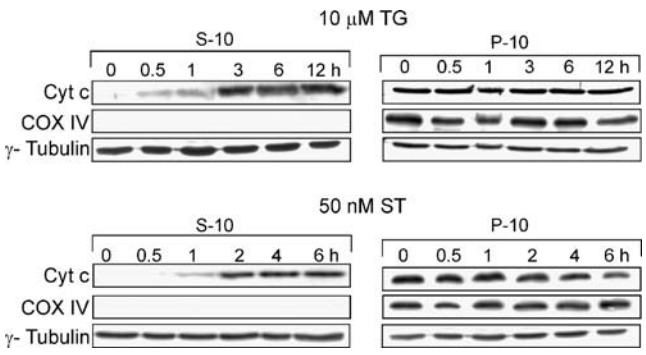

Fig. 2 Effect of mitochondrial damage inducers on mitochondrial release of cyt c. Samples from the cellular fractions S-10 and P-10 were subjected to Western blotting and chemiluminescent reaction for detecting cyt c (p12), COX IV (19.6) and γ-tubulin (p48). S-10 was the supernatant once the cells were treated with digitonin and centrifuged at 10,000 ×g for 10 min. P-10 was the soluble content of the low speed pellet enriched in nuclei and mitochondria

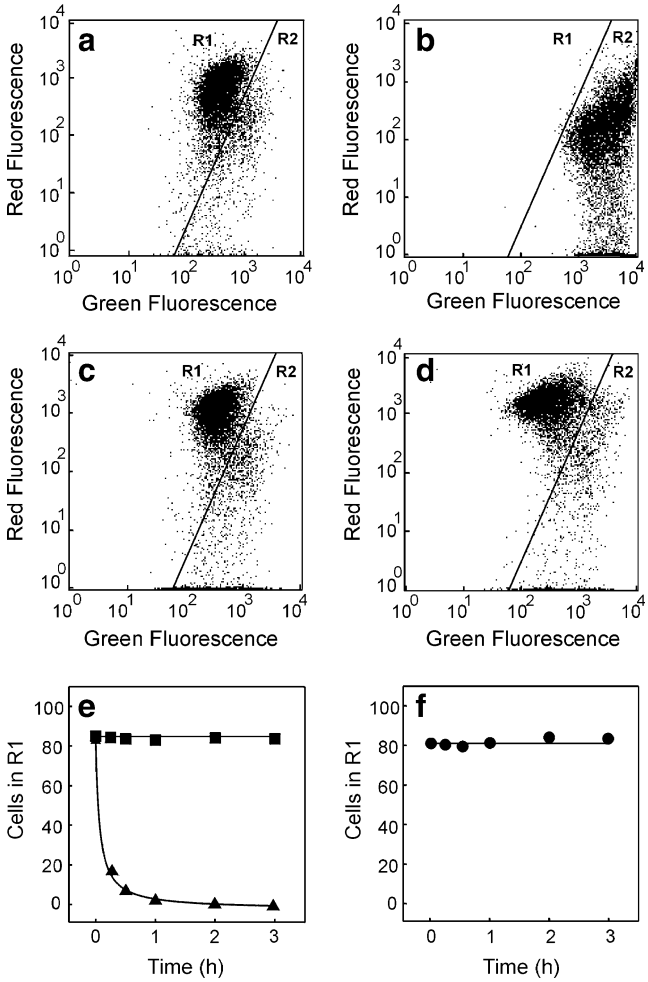

Fig. 3 Effect of mitochondrial damage inducers on $\Delta\Psi_m$ as detected by flow-cytometry. Treated and untreated cells were loaded with JC-1 before measurements. After appropriate electronic gating, the green and red fluorescence of JC-1 was detected through the FL-1 and FL-2 channel, respectively. Dots plot of untreated cells (**a**), cells exposed to 10 μM TG for 2 h (**b**), cells preincubated for 10 min with 5 μM CsA before the 2 h treatment with 10 μM TG (**c**), or cells treated for 2 h with 50 nM ST (**d**). Effect of the 10 μM TG treatment as a function of time (**e**) in the absence (closed triangles) or presence of a 10 min preincubation with 5 μM CsA (closed squares). Time dependent effect when cells were exposed to 50 nM ST (**f**)

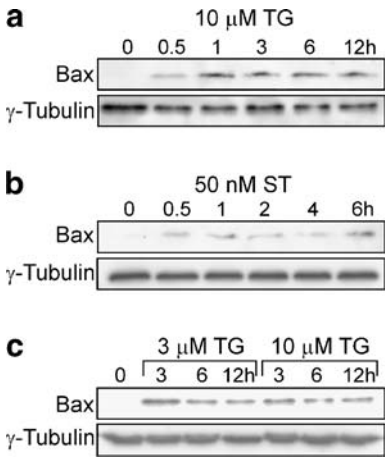

Fig. 4 Effect of mitochondrial damage inducers on Bax translocation. Samples before or after the indicated time of treatment were processed for immunodetection of active Bax (p21) in the corresponding P-10 fraction. Effect induced by the addition of 10 μM TG (**a**), or 50 nM ST (**b**). Comparative effect when 3 or 10 μM TG was added (**c**). Blots were reprobed to detect γ-tubulin (p48) in each lane

Thus, the addition of 10 μM TG to the cells was followed by an early loss of $\Delta\Psi_m$ and this effect could be prevented by cells preincubation with CsA (Fig. 3e). In contrast, the addition of 50 nM ST had no impact on $\Delta\Psi_m$ at least during the first 3 h of exposure (Fig. 3f).

Bax is a pro-apoptotic protein of the Bcl-2 family that has been involved in permeabilization of the OMM and release of apoptotic proteins including cyt c (Jürgensmeier et al. 1998; Eskes et al. 1998). Bax detection in the P-10 fraction was performed by Western blotting using the monoclonal antibody 6A7 (Tikhomirov and Carpenter 2005). The γ-tubulin content was also evaluated to ensure that samples to be compared had similar amounts of protein. The Bax protein was absent in the P-10 fraction before treatment with 10 μM TG but was detected after the TG addition (Fig. 4a). The immunoreactive band was visible at 30 min and was present even after 12 h. Bax translocation to mitochondria was also detected when cells were treated with 50 nM ST (Fig. 4b). The appearance of Bax in the P-10 fraction was observed after 30 min of treatment. In order to identify the origin of the TG-induced mitochondrial Bax, cells were subjected to treatment with either 3 or 10 μM TG for different time periods. Comparative assessment of mitochondrial Bax was pursued by running and processing simultaneously samples of both treatments and loading equal amounts of protein in the lanes. As can be seen, Bax levels in the P-10 fraction after addition of 3 μM TG were very similar to those observed when 10 μM TG was added (Fig. 4c).

Casp 3 is a key mediator in the execution of certain downstream events when the apoptotic process is triggered by mitochondrial damage (Slee et al. 1999; Lakhani et al. 2006). The initial processing of pro-casp 3 that is usually after Asp^{175} produces the large subunit with the pro-domain (p24) and the small subunit (p12). A further cleavage of the larger fragment at Asp^{9} generates the p20 fragment that can be processed at Asp^{28} to produce the accumulation of p17 (Chandra and Tang 2003). Cells treatment with 10 μM TG resulted in casp 3 activation as detected by the presence of the p17 fragment in the S-10 fraction. The accumulation of p17 was clear after 3 h of treatment (Fig. 5a). Parallel

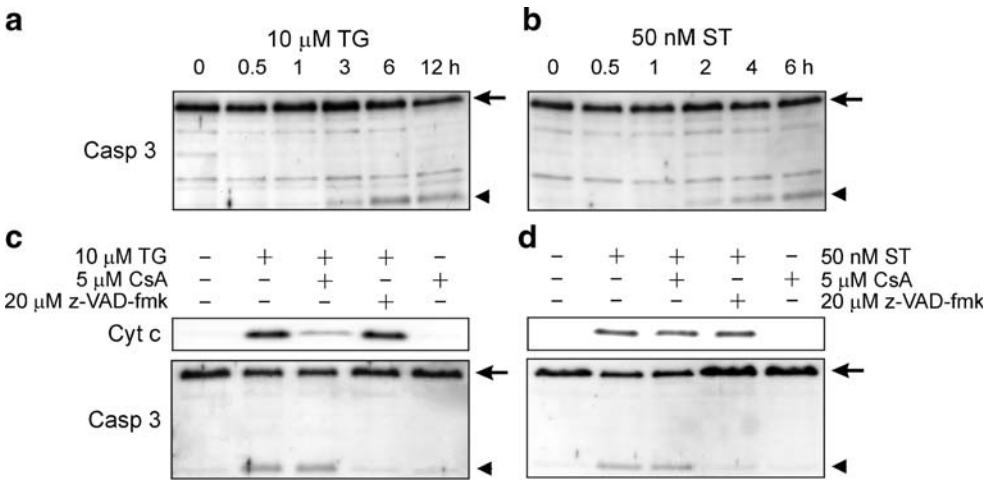

Fig. 5 Casp 3 activation and effect of CsA or z-VAD-fmk on apoptotic mediators after mitochondrial damage. The S-10 fraction of treated or untreated cells was used for casp 3 and cyt c detection by Western blotting. Time dependent effect of 10 μM TG (**a**) or 50 nM ST (**b**) on casp 3 activation. Cyt c and casp 3 were also studied when cells were subjected to: no treatment; treatment for 6 h with 10 μM TG; preincubation for 10 min with 5 μM CsA before the 10 μM TG treatment or preincubation for 1 h with 20 μM z-VAD-fmk before the 10 μM TG treatment (**c**). Detection of cyt c and casp 3 when cells were exposed to 50 nM ST for 6 h (**d**) as described for the TG treatment. Pro-casp 3 (p32) is marked with arrow and the cleaved fragment (p17) with arrowhead

experiments using 50 nM ST as inducer of mitochondrial damage provided a similar result. In this case, the p17 fragment subsequent to pro-casp 3 cleavage was detected after 2 h of ST treatment (Fig. 5b).

The mechanisms of cyt c release and casp 3 activation were then analyzed with the aid of the PTP opening blocker CsA and the general caspase inhibitor z-VAD-fmk. As already shown, 6 h treatment with 10 μM TG produced accumulation of cyt c in the S-10 fraction (Fig. 5c; see also Fig. 2). However, the accumulation of cyt c was substantially lowered but not totally eliminated when cells were preincubated for 10 min with 5 μM CsA. In contrast, cells preincubation for 1 h with 20 μM z-VAD-fmk was ineffective in preventing the TG-induced release of cyt c. It is also shown that cells preincubated with 5 μM CsA alone did not induce any response. Regarding casp 3, the accumulation of p17 fragment in the S-10 fraction was clearly observed after the 6 h treatment with 10 μM TG (Fig. 5c; see also panel a). Moreover, the TG-induced activation occurred even when cells were preincubated for 10 min with 5 μM CsA but was drastically inhibited when cells were preincubated for 1 h in the presence of 20 μM z-VAD-fmk. No effect on casp 3 activation was observed by the CsA addition to untreated cells. Furthermore, incubation with 50 nM ST for 6 h caused accumulation of cyt c in the S-10 fraction that was unaltered when cells were preincubated for 10 min with 5 μM CsA or after 1 h preincubation in the presence of 20 μM z-VAD-fmk (Fig. 5d). In this case, no quantitative difference was observed in the accumulated cyt c when either CsA or z-VAD-fmk was added in preincubation. Likewise, the ST treatment induced casp 3 activation when cells were preincubated with CsA but not when cells were preincubated with z-VAD-fmk (Fig. 5d).

Comparative measurements indicated that the accumulation of cyt c in S-10 at several time intervals after the 10 μM TG addition was similar to that observed when 50 nM ST was used (Fig. 6a and b). Nonetheless, the release induced by 10 μM TG was considerably higher than that induced by 3 μM TG (Fig. 6c and d). Interestingly, cyt c accumulated after the 10 μM TG treatment was similar to that induced by 3 μM TG when cells were preincubated for 10 min with 5 μM CsA (Fig. 6e and f).

When phase contrast images were taken before and after the mitochondrial damage it was observed that cell morphology was clearly altered after 30 min exposure to 50 nM ST but was unaffected when the 30 min incubation was carried out in the presence of 10 μM TG (Fig. 7, first row). The effect of TG on cell morphology was only observed after 2 h (data not shown). On the other hand, fluorescence microscopy revealed that cells exposure to 50 nM ST for 1 h was enough to develop a robust nuclear condensation (Fig. 7, second row) and prolongation of the

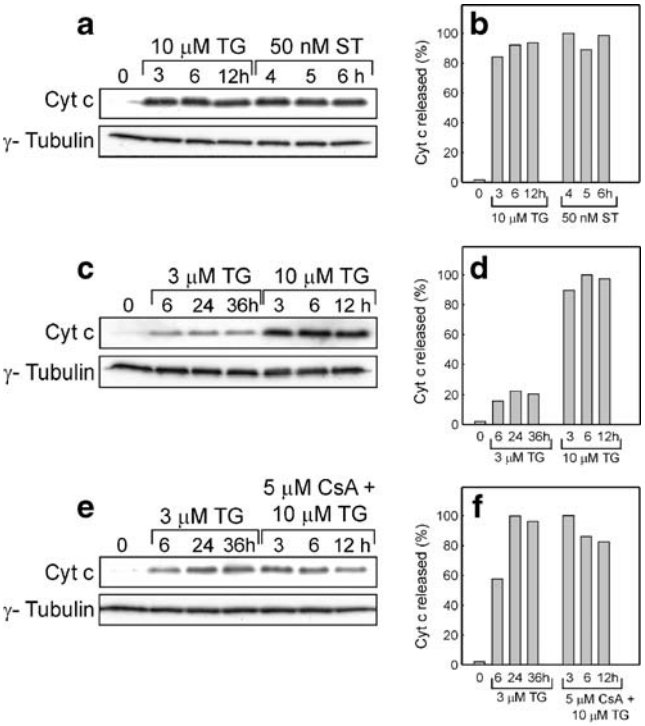

Fig. 6 Evaluation of cyt c when cells were subjected to different treatments. Cyt c (p12) was detected by Western blotting in the S-10 fraction. Cells were treated with 10 μM TG vs. 50 nM ST (**a** and **b**). Cells were treated with 3 μM TG vs. 10 μM TG (**c** and **d**). Effect of 3 μM TG vs. 10 μM TG when preceded by 10 min preincubation with 5 μM CsA (**e** and **f**). Blot reprobing was carried out for γ-tubulin (p48) detection in each lane. Cyt c levels detected by densitometry were normalized against the corresponding γ-tubulin content and expressed in a relative scale (**b**, **d** and **f**)

treatment for up to 2 h displayed a similar response. However, spindle-shaped cells and chromatin staining were unaltered after 1 h treatment with 10 μM TG (Fig. 7, third row) although progressive rounding of the cells and condensed nuclei were evident after 2 h exposure. It is also shown that 1 h preincubation with 20 μM z-VAD-fmk before exposure to 50 nM ST for 1 or 2 h was clearly unable to prevent chromatin condensation (Fig. 7, last row).

Discussion

When the mitochondrial dysfunction was evaluated by reduction of the tetrazolium dye MTT it was clear that either 10 μM TG or 50 nM ST exerted a rapid noxious effect on H9c2 cells (Fig. 1). The alteration induced by TG or ST on mitochondria was confirmed by the early release of cyt c (Fig. 2).

Mitochondrial damage is usually associated with accumulation of cyt c into the cytosol and collapse of $\Delta\Psi_m$ even though the relationship between both parameters is a matter

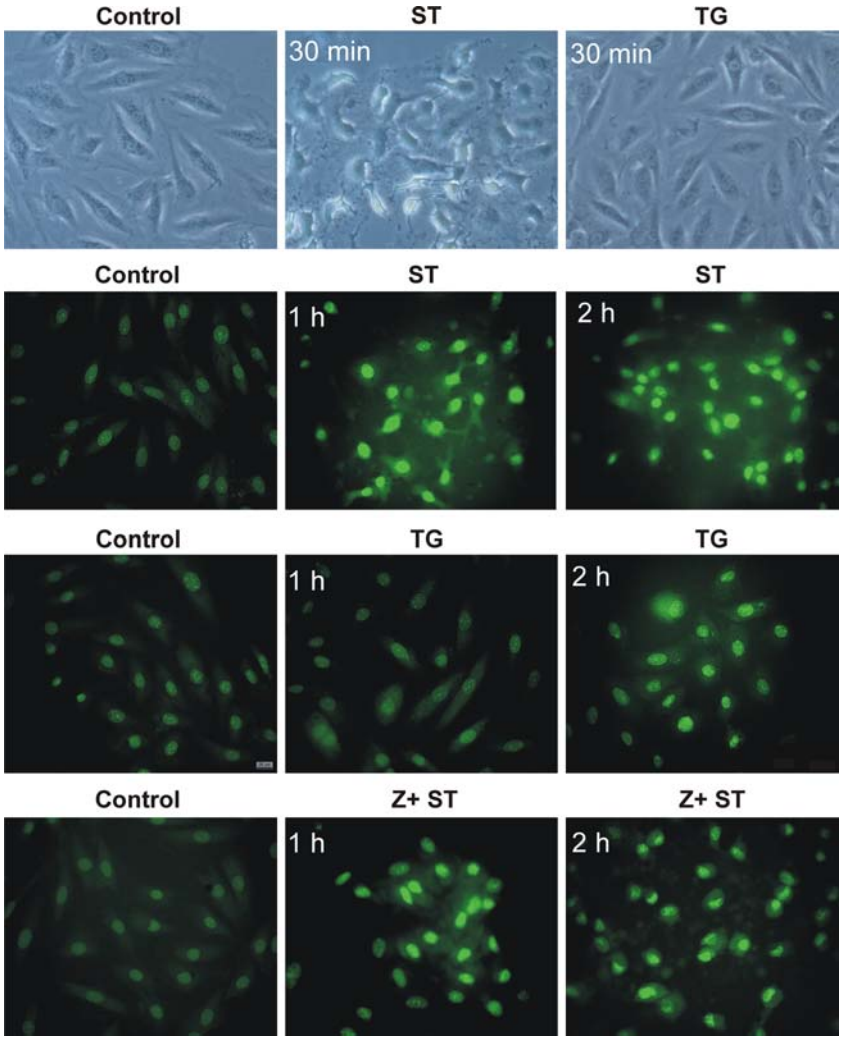

Fig. 7 Microscopy images when plated cells were exposed to mitochondrial damage inducers. Phase contrast before or after 30 min treatment with 50 nM ST or 10 μM TG (first row). Fluorescence of AO-stained chromatin before or after the following treatments: 1 or 2 h with 50 nM ST (second row), 1 or 2 h with 10 μM TG (third row), 1 or 2 h with 50 nM ST preceded by 1 h preincubation with 20 μM z-VAD-fmk (Z) (fourth row)

of controversy. For instance, the mitochondrial release of cyt c preceded and was independent of $\Delta\Psi_m$ when human T lymphoblastoid cells were exposed to 1 μM ST (Bossy-Wetzel et al. 1998). However, cyt c release occurred as a consequence of rapid $\Delta\Psi_m$ dissipation when rat pheochromocytoma-6 cells were treated with 5 μM ST (Heiskanen et al. 1999). Our data indicated that cyt c release induced by 10 μM TG (Fig. 2) was linked to rapid collapse of $\Delta\Psi_m$ (Fig. 3e) whereas that induced by 50 μM ST was initiated before any detectable loss of $\Delta\Psi_m$ was observed (cf. Figs. 2 and 3f). It is clear that TG and ST acting on the same cell model gives rise to different mechanisms of cyt c release. It is also true that different concentrations of the same apoptotic inducer acting on the same cell model may elicit different responses. This is illustrated by the release of cyt c induced by 10 μM TG that was associated to fast $\Delta\Psi_m$ decrease (Figs. 2 and 3) whereas that triggered by 3 μM TG occurred without any effect on $\Delta\Psi_m$ (Soler et al. 2007).

The extent of cyt c release induced by 10 μM TG was larger than that induced by 3 μM TG (Fig. 6c and d) but was coincident with that induced by 3 μM TG when cells were preincubated with CsA before the 10 μM TG treatment (Fig. 6e and f). In addition, the release of cyt c induced by 10 μM TG was in a large extent but not totally sensitive to CsA (Fig. 5c; see also Fig. 6e and f). Therefore, the larger component of cyt c induced by 10 μM TG was CsA-sensitive and can be attributed to irreversible PTP opening and collapse of $\Delta\Psi_m$. The smaller component was CsA-insensitive (Fig. 6e and f) and corresponded to cyt c release taking place in the absence of mitochondria depolarization (Soler et al. 2007). It should be considered that the 10 μM TG treatment evoked a rapid and direct effect on mitochondria that was superimposed to a slower and indirect effect induced by inhibition of the sarcoplasmic reticulum Ca^{2+}-ATPase. The latter effect can be evaluated when a lower TG concentration such as 3 μM is used (Soler et al. 2007). In contrast, the release of mitochondrial cyt c induced by 50 nM ST was totally insensitive to CsA (Fig. 5d).

Comparative measurements indicated that Bax levels in the P-10 fraction induced by 10 μM TG were similar to

those observed when 3 μM TG was used (Fig. 4c). This suggests that 10 μM TG did not induce any additional Bax translocation to the mitochondria with respect to that triggered by 3 μM TG. Therefore, early release of cyt c induced by 10 μM TG (Fig. 2) was associated to rapid collapse of $\Delta\Psi_m$ (Fig. 3e) and occurred without participation of Bax. In marked contrast, the release of cyt c during the 50 μM ST treatment was caused by the Bax protein leading to permeabilization of the OMM in the absence of mitochondria depolarization (Fig. 3f).

Otherwise, treatment with 10 μM TG or 50 nM ST accumulated similar levels of cyt c in the cytosol (Fig. 6a and b). This suggests that PTP opening associated to rapid loss of $\Delta\Psi_m$ does not release more cyt c than selective permeabilization of the OMM.

Furthermore, time-dependent activation of casp 3 was observed under the presence of TG or ST (Fig. 5a and b) in a process that was sensitive to z-VAD-fmk (Fig. 5c and d). However, the release of mitochondrial cyt c induced by either 10 μM TG or 50 nM ST was independent on caspase activation (Fig. 5c and d). This indicates that cyt c release occurs upstream of casp 3 processing.

The earlier mitochondrial damage developed in the presence of TG when compared with that induced by ST (Fig. 1) can be correlated with the time course of cyt c release (Fig. 2). However, visualization of the cell culture indicated that morphological alterations of the cell were developed earlier under the presence of ST (Fig. 7, first row). Indeed, protein detection by Western blotting was impossible to perform when cells were exposed for more than 6 h to ST but not to TG (data not shown). Chromatin condensation was subsequently observed and the effect of ST was also developed earlier (Fig. 7, second row) when compared with TG (Fig. 7, third row). More importantly, cells preincubation with z-VAD-fmk did not protect against chromatin condensation induced by the ST treatment (Fig. 7, fourth row). This can be explained by the existence of a very active caspase-independent death mechanism induced by ST (Déas et al. 1998; Belmokhtar et al. 2001).

In conclusion, the mitochondrial disturbance that makes H9c2 cells highly sensitive to apoptotic death was directly related with kinetics of cyt c release in a process that may or may not be linked to mitochondrial depolarization. However, earlier mitochondrial dysfunction as that induced by TG, when compared with ST, did not correlate with earlier structural alterations. The lack of correspondence between biochemical apoptotic parameters and structural changes of the cells has been previously recognized (Galluzzi et al. 2007). This is consistent with redundant pathways and compensatory mechanisms that seem to be involved in the non-physiological death of cardiac myocytes.

Acknowledgements This study was supported by grant BMC2002-02474 from Ministerio de Educación y Cultura, Spain and by a grant-in-aid from the Universidad de Murcia.

References

Belmokhtar CA, Hillion J, Ségal-Bendirdjian E (2001) Oncogene 20:3354–3362
Bernardi P, Scorrano L, Colonna R, Petronilli V, Di Lisa F (1999) Eur J Biochem 264:687–701
Bossy-Wetzel E, Newmeyer DD, Green DR (1998) EMBO J 17:37–49
Chandra D, Tang DG (2003) J Biol Chem 278:17408–17420
Cossarizza A, Baccarani-Contri M, Kalashnikova G, Franceschi C (1993) Biochem Biophys Res Comm 197:40–45
Déas O, Dumont C, McFarlane M, Rouleau M, Hebib C, Harper F, Hirsch F, Charpentier B, Cohen GM, Senik A (1998) J Immunol 161:3375–3383
Eskes R, Antonsson B, Osen-Sand A, Montessuit S, Richter C, Sadoul R, Mazzei G, Nichols A, Martinou JC (1998) J Cell Biol 143:217–224
Ferri KF, Kroemer G (2003) BioEssays 23:111–115
Galluzzi L, Maiuri MC, Vitale I, Zischka H, Castedo M, Zitvogel L, Kroemer G (2007) Cell Death Differ 14:1237–1243
Garrido C, Galluzzi L, Brunet M, Puig PE, Didelot C, Kroemer G (2006) Cell Death Differ 13:1423–1433
Goldstein JC, Waterhouse NJ, Juin P, Evan GI, Green DR (2000) Nat Cell Biol 2:156–162
Goldstein JC, Muñoz-Pinedo C, Ricci J-E, Adams SR, Kelekar A, Schuler M, Tsien RY, Green DR (2005) Cell Death Differ 2:453–462
Gottlieb RA, Granville DJ (2002) Methods 26:341–347
Green DR, Kroemer G (2004) Science 305:626–629
Heiskanen KM, Bhat MB, Wang H-W, Ma J, Nieminen A-L (1999) J Biol Chem 274:5654–5658
Jürgensmeier JM, Xie Z, Deveraux Q, Ellerby L, Bredesen D, Reed JC (1998) Proc Natl Acad Sci USA 95:4997–5002
Kimes BW, Brandt BL (1976) Exp Cell Res 98:367–381
Korge P, Weiss JN (1999) Eur J Biochem 265:273–280
Kroemer G, Reed JC (2000) Nat Med 6:513–519
Lakhani SA, Masud A, Kuida K, Porter GA Jr, Booth CJ, Mehal WZ, Inayat I, Flavell RA (2006) Science 311:847–851
Lax A, Soler F, Fernandez-Belda F (2005) J Bioenerg Biomembr 37:249–259
Lax A, Soler F, Fernandez-Belda F (2006) Biochim Biophys Acta 1763:937–947
Regula KM, Ens K, Kirshenbaum LA (2003) J Mol Cell Cardiol 35:559–567
Rossner M, Yamada KM (2004) J Cell Biol 166:11–15
Sagara Y, Inesi G (1991) J Biol Chem 266:13503–13506
Scorrano L, Ashiya M, Buttle K, Weiler S, Oakes SA, Mannella CA, Korsmeyer SJ (2002) Dev Cell 2:55–67
Slee EA, Harte MT, Kluck RM, Wolf BB, Casiano CA, Newmeyer DD, Wang H-G, Reed JC, Nicholson DW, Alnemri ES, Green DR, Martin SJ (1999) J Cell Biol 144:281–292
Smith PK, Krohn RI, Hermanson GT, Mallia AK, Gartner FH, Provenzano MD, Fujimoto EK, Goeke NM, Olson BJ, Klenk DC (1985) Anal Biochem 150:76–85
Soler F, Lax A, Fernandez-Belda F (2007) Arch Biochem Biophys 466:194–202
Tikhomirov O, Carpenter G (2005) J Cell Sci 118:5681–5690
Vercesi AE, Moreno SNJ, Bernardes CF, Meinicke AR, Fernandes EC, Docampo R (1993) J Biol Chem 268:8564–8568